The influence of paper surface sizing on inkjet pigment penetration

TIAGO G. COSTA[1], JOSÉ A. GAMELAS[2*], ISABEL M. MOUTINHO[3], M. MARGARIDA FIGUEIREDO[4], PAULO J. FERREIRA[5]

SUMMARY

The effect of paper surface sizing on inkjet pigment penetration was evaluated by studying four different paper samples: one taken as reference, without surface sizing (paper RP), one surface sized with cationic starch (RPS1), one with a mixture of cationic starch and poly(styrene-co-maleic anhydride) (RPS2), and one with a mixture of cationic starch and poly(styrene-co-acrylate) (RPS3). Assessment was based on the grey level analysis of a black printed area on the top surface of the paper samples and on internal layers below that printed area (obtained by delamination of the paper sheets). From the grey level distribution curves it was possible to confirm that the majority of the ink was retained at the top surface, as expected. The penetration degree of the ink pigment was RPS1 < RPS3 << RPS2 << RP and the results were found to be related to the polar component of the surface energy. The ink penetration into the paper sheets was less pronounced for the papers with a higher surface polar character due to the stronger interactions between the water based ink and the surface sizing agents. The highest ink penetration was observed for sample RP due to the very low polarity (and lower topographical uniformity) of its surface.

KEYWORDS
surface sizing, ink pigment, image analysis, inkjet printing, paper

INTRODUCTION

The interaction of ink components with the paper surface and the corresponding degree of penetration into the paper structure has important effects on printing quality. During the printing process with pigment-based inks, the pigment should separate from the ink vehicle (usually water in inkjet printing and vegetable or mineral oils in offset printing) and should also be preferentially retained at the paper surface. On the other hand, the penetration of the ink vehicle should be minimized, in order to prevent the reduction of the paper sheet strength properties or the loss of opacity. Weak ink pigment retention at the paper surface (with correspondingly high penetration into the paper sheet) produces low optical densities and high print through (the visibility of the printed area on the reverse side of the paper) and, consequently, a low printing quality (*1-5*).

Several studies have been made regarding the interaction of the ink pigments with the paper structure in both inkjet (*1,2,6-13*) and offset printing (*3-5,14*). In particular, Eriksen and Gregersen used images from scanning electron microscopy to assess the position, in the Z direction of the paper sheet, of the pigments of a yellow coldset offset ink, and a specially made white ink (with TiO_2 as ink pigment) (*3,4*). The study was made with TMP-based sheets, to which different amounts of chemical pulp and fines were added. The depth of penetration determined using the microscopy-based method was no larger than 5 µm in all samples. A reduction of the penetration depth with increasing amount of fines (due to the higher retention of the ink pigments at the surface) and with calendaring was found. The same authors also studied the penetration of a black coldset offset ink and different mixtures of ink oils again in commercial TMP-based papers using sheet splitting techniques (delamination), and reflectance measurements on the surfaces of the obtained layers (*5*). With this method, they found that the penetration of the oils and the black ink into the paper sheets was deeper than 40 µm (more than 40% of the total paper thickness). As for the penetration of inkjet pigments into the paper structure no studies could be found in the open literature.

Surface sizing is used to control some relevant paper surface properties such as porosity, roughness and surface chemistry, in order to promote an adequate interaction with inks and to improve the final printing quality (*15-19*). This operation may involve application of cationic starch alone or by combining it with synthetic polymers (*17-19*). In a previous study (*20*), the authors found, by using FT-IR on surface sized, uncoated *E. globulus* kraft pulp based papers, that surface sizing agents, including cationic starch, poly(styrene-co-maleic anhydride) and poly(styrene-co-butyl acrylate), are mostly located at the top surface. The depth of penetration of the sizing materials into the paper structure was less than 30% of the paper thickness. The study of the effect of surface sizing, particularly the interaction of the sizing formulations with the base paper and with the inks is, thus, of utmost importance. In the present study, the effect of surface sizing agents on the penetration degree of a black inkjet ink was considered by varying the surface sizing materials and after printing, determining the grey level values of the printed areas and of the corresponding areas in the layers below (*21*).

EXPERIMENTAL

Materials

Four paper samples were studied: a calendered uncoated base paper (RP, denoting "reference sample") produced with a *E. globulus* Kraft pulp, and three samples obtained after surface sizing the base paper in laboratory, with cationic starch (formulation S1) and with two mixtures of cationic starch and a copolymer (in a proportion of 90/10 w/w), as summarized in Table 1. Cationic starch has a few C6 positions substituted by 2-hydroxy-3-trimethylammoniumpropyl groups (substitution degree of about 0.03). The copolymers have the structures depicted in Figure 1, as deduced from the elemental analysis measurements (*19*).

The surface sizing formulations were applied using a Mathis laboratory coating device, SVA-IR-B (*20*). A 0.15 mm roll was used and its velocity adjusted to 6

[1]Master Student, [2]Research Scientist and corresponding author (jafgas@eq.uc.pt), [3]PhD Student, [4]Full Professor, [5]Auxiliary Professor
Departamento de Engenharia Química
Universidade de Coimbra, Pólo II – R. Sílvio Lima
3030-790 Coimbra, Portugal.

Table 1
Paper surface sizing

Chemical formulations used in the surface sizing	Paper samples
---	Reference paper, RP
cationic starch, **S1**	RPS1
cationic starch/ poly(styrene-co-maleic anhydride), 90:10 (w/w), **S2**	RPS2
cationic starch/ poly(styrene-co-acrylate), 90:10 (w/w), **S3**	RPS3

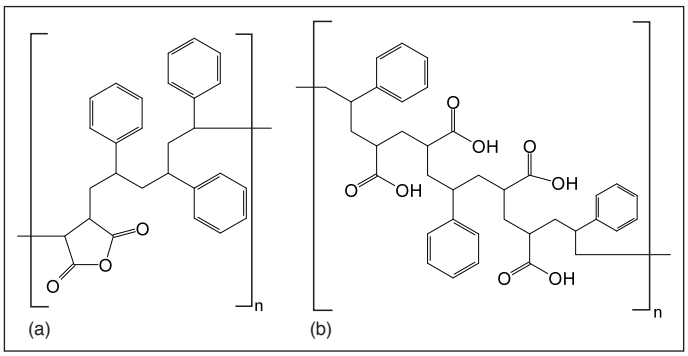

Fig. 1 Chemical structure of poly(styrene-co-maleic anhydride) (a), and poly(styrene-co-acrylate) (b).

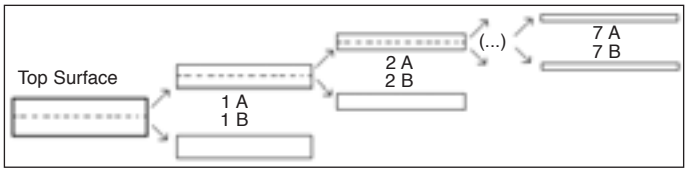

Fig. 2 Schematic representation of the paper delamination process.

m/min. The drying process was performed in two steps: first with an IR drier coupled to the applicator roll using a 1.0 kW drying intensity, and next with air drying for at least 10 min. The total surface sizing pick-up (in both paper surfaces) was 3.5 ± 0.3 g/m^2. The surface sized samples were not calendered.

The contact angles with water and organic liquids with known surface tensions (formamide, ethylene glycol, propylene glycol) were measured with the DataPhysics OCA20 equipment using the sessile drop method, as previously reported (*22*), and the surface energy parameters were then determined by using the Owens and Wendt model (*23*). The sample porosities were determined using a mercury porosimeter AutoPore IV 9500 from Micromeritics. The principles of the technique and its use in paper samples are detailed elsewhere (*24*).

Print assessment methods

A black rectangle of 29×19 mm^2 was printed on each paper sample using a HP Deskjet 6540 operating at the maximum printing quality mode. A pigment-based black ink was used (HP C8765E). After printing, each paper sheet was split into different layers, by delamination, as follows:

(1) each sample was coated on both sides with a 125 µm thickness sheet of plastic using the Leitz PH 9 Photo Laminator 4B device;
(*2*) the paper sheet was then divided in two layers originating two new surfaces, the upper layer (1A) and the layer below (1B);
(*3*) steps 1 and 2 were repeated for the upper layer, originating again two new surfaces, (2A) and (2B);
(*4*) the same procedure was repeated several times in order to generate surfaces 3B, 4B, 5B, 6B and 7B.

This procedure is schematically detailed in Figure 2. The thickness of the samples obtained by the paper samples delamination process was measured using an Optical Microscope Olympus BH-2.

Images of the top surface, containing the printed area and of the corresponding surfaces obtained by delamination (namely 1B, 2B, 3B, 4B, 5B, 6B and 7B) were acquired in the reflective mode using an Epson Perfection V500 Photo scanner. The resolution for the image acquisition was 2400 dpi and the assessed area was 31×22 mm^2, slightly larger than the black printed rectangle area, in order to use the unprinted areas for the background correction, as explained below. Figure 3 shows the images corresponding to the reference paper.

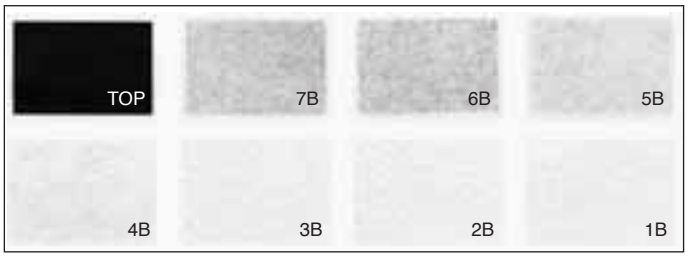

Fig. 3 Images for the reference paper of the printed area (top) and of the corresponding surfaces obtained by delamination.

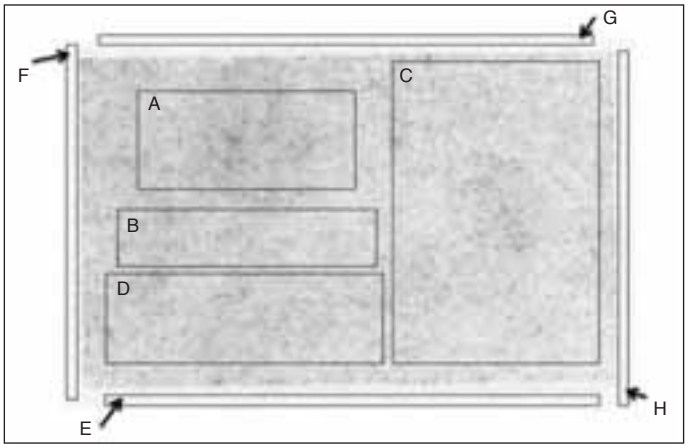

Fig. 4 Illustration of the areas used for the scanning assessment.

The 8 bits (tiff) digital images from the scanner were exported to the ImageJ software in order to obtain the grey level histograms. Typically, for each digital image, four grey level measurements were made in randomly selected regions (A, B, C and D) of the 29×19 mm^2 printed area, as illustrated in Figure 4. An average histogram such as the example depicted in Figure 5(a) was obtained. Background correction was applied by taking four measurements in the "white" regions outside the printed area (E, F, G and H), and subtracting the resultant average histogram (such as the example in Fig. 5(b)) from the histogram of Figure 5(a). The final result is a histogram similar to that plotted in Figure 5(c).

This procedure was repeated for each paper sample in two additional printed areas. Several statistical parameters

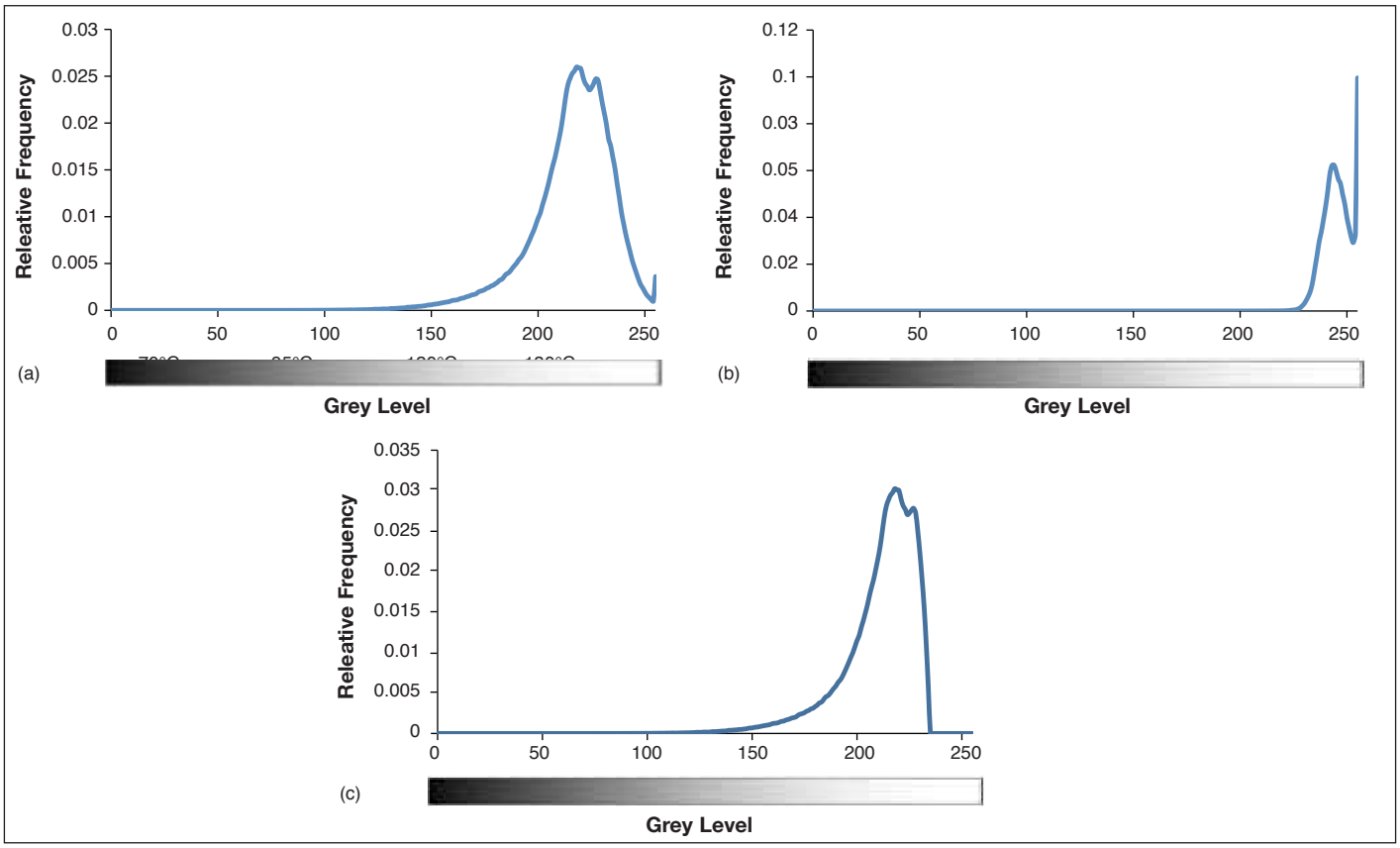

Fig. 5 Grey level histograms for the uncoated base paper (inner layer surface 3B): (a) printed area; (b) white area; (c) as (a) subtracted from (b).

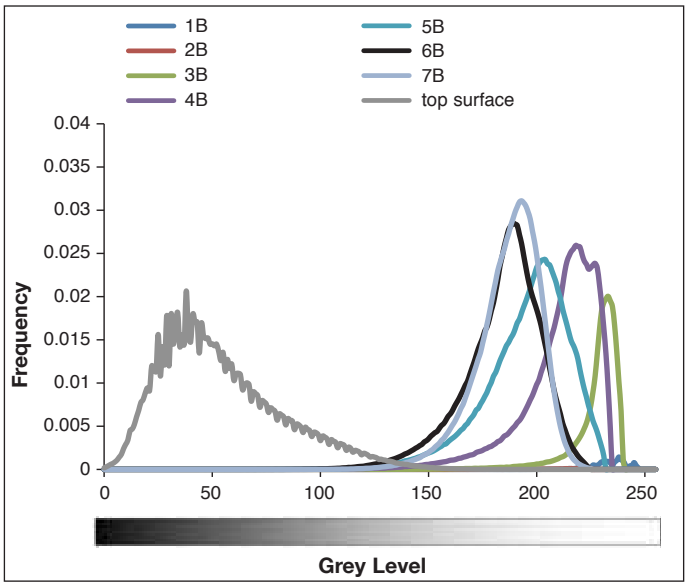

Fig. 6 Grey level histograms for the uncoated base paper.

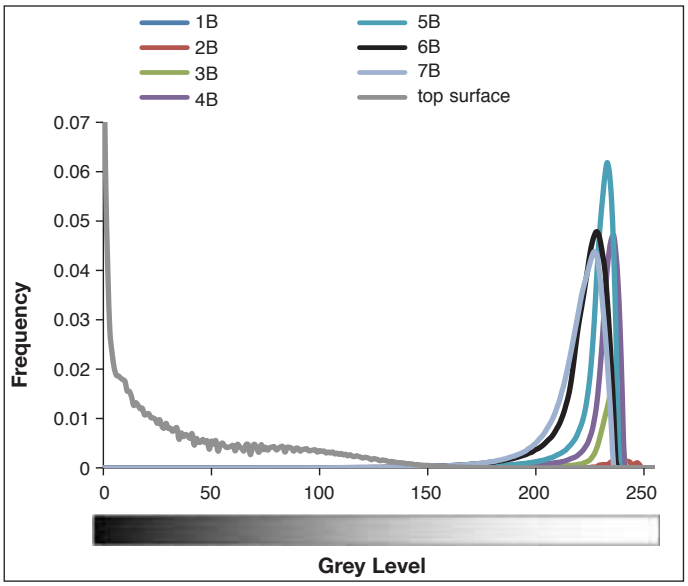

Fig. 7 Grey level histograms for the paper surface sized with cationic starch.

including the mean, median, standard deviation and skewness, were computed by processing the data of the histograms in Matlab R2007B.

RESULTS AND DISCUSSION

1. Grey level histograms analysis

Grey level distribution curves were obtained for the four paper samples studied, at the top surface and at the surfaces obtained by the delamination process (surfaces 1B to 7B as detailed in Fig. 2). Figures 6, 7 and 8 include the curves corresponding to the uncoated base paper (sample RP), the paper sized only with cationic starch (sample RPS1) and the paper sized with cationic starch and copolymer (sample RPS2), respectively. The most relevant statistic parameters such as the mean, median, standard deviation and skewness of each histogram are listed in Table 2 for all the samples and for all the layers.

From these figures, it is obvious that the grey level distribution curves corresponding to the top surfaces are towards the left and approach the "black" levels (grey levels near 0) whereas those corresponding to the inner layer surfaces are towards the right and approach the

Table 2
Results for the grey level parameters at different depths of printed paper samples

		Depth %	Depth µm	Mean	Median	Standard Deviation	Skewness
RP	Top	0	0	54	49	28.4	0.83
	7B	21	24	188	189	14.8	-0.86
	6B	32	36	184	187	17.8	-0.89
	5B	40	46	196	199	19.3	-0.93
	4B	50	58	211	215	17.5	-1.60
	3B	58	66	228	231	11.0	-2.64
	2B	68	78	217	218	5.4	-0.15
	1B	81	93	234	235	7.3	-0.46
RPS1	Top	0	0	41	26	38.8	0.97
	7B	15	17	219	222	14.0	-2.32
	6B	23	25	221	225	14.5	-2.73
	5B	32	34	228	231	10.6	-3.35
	4B	44	48	231	234	9.8	-3.68
	3B	55	59	232	234	9.1	-3.53
	2B	63	68	239	239	5.4	-0.17
	1B	78	84	221	217	8.1	0.68
RPS2	Top	0	0	47	39	30.8	0.91
	7B	20	24	209	213	15.3	-1.84
	6B	28	34	217	220	14.0	-2.09
	5B	35	42	220	224	13.6	-2.46
	4B	45	54	227	230	11.2	-2.96
	3B	57	69	229	232	11.5	-2.94
	2B	67	81	231	231	4.7	-0.79
	1B	78	94	232	233	6.7	-0.73
RPS3	Top	0	0	45	35	34.9	0.91
	7B	13	22	217	220	13.0	-2.22
	6B	25	35	220	224	13.5	-2.56
	5B	34	47	227	229	10.4	-3.20
	4B	43	58	230	232	8.4	-3.70
	3B	53	67	234	235	5.3	-2.50
	2B	65	76	230	231	3.7	-1.46
	1B	78	88	232	233	5.9	-0.61

"white" levels (grey levels near 255). This drastic reduction in colour intensity means that the penetration is not extensive and thus most of the ink pigment is retained at the surface. As expected, the inner layers furthest from the top surface, show grey level distribution curves closest to the "white" level.

Besides this common general behaviour, important differences in the performance of the paper samples regarding ink penetration can be detected in the histograms. For instance, clear differences can be found when comparing the data obtained for the reference paper (Fig. 6) to those from the surface sized samples (cationic starch (Fig. 7) and cationic starch/poly(styrene-co-maleic anhydride) (Fig. 8)). Besides some discrepancies among the grey level distributions at the top surface, it is noteworthy that the curves corresponding to the various surfaces of the internal layers are closer to each other and more shifted towards the "white" level for the sized papers. Moreover, differences can also be detected between the samples sized with different formulations.

Comparing the results for the top surface (Fig. 9), it is apparent that the frequency near zero level ("black") is considerably higher for the paper sample RPS1, suggesting, in this case, a higher retention of ink at this surface in comparison to the other samples. Similarly, the mean grey level value at the top surface is also considerably lower for RPS1 than for the other samples (Table 2). The largest mean grey level value is obtained for sample RP.

This is in agreement with the grey level distribution curves obtained for the inner layer surface closest to the top surface, 7B (Fig. 10), which clearly show that the sample in which the ink has penetrated most is the reference paper, with RPS1 the one whose curve is more displaced to the "white" levels. The samples RPS2 and RPS3 show an intermediate behaviour between samples RP and RPS1. In general, the histograms at the inner layer surfaces 6B to 1B exhibit the

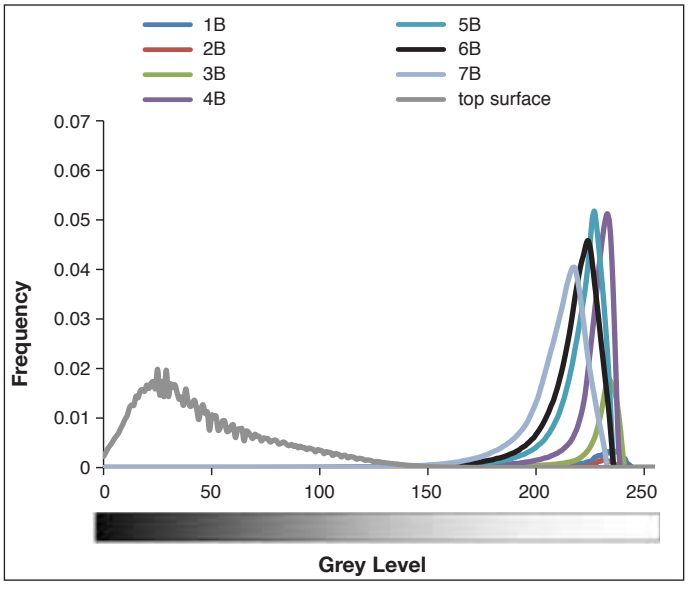

Fig. 8 **Grey level histograms for the paper surface sized with cationic starch/poly(styrene-co-maleic anhydride).**

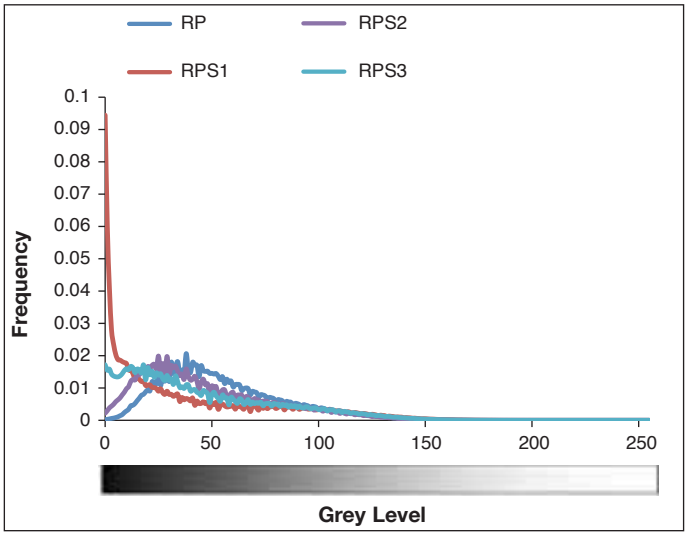

Fig. 9 **Grey level histograms at the top surface for the distinct samples.**

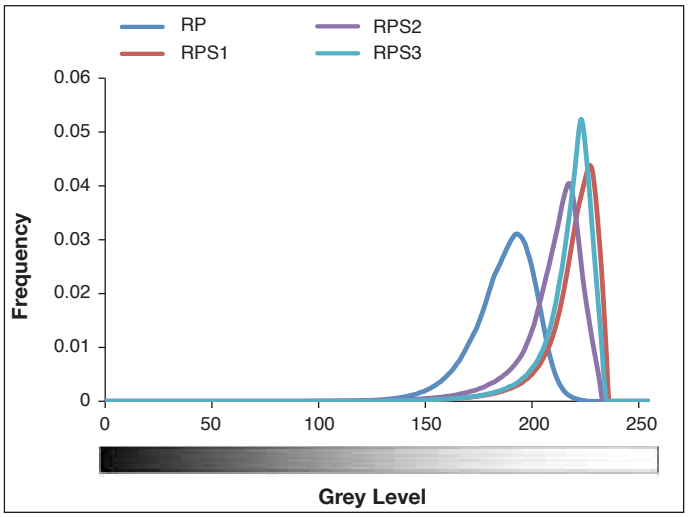

Fig. 10 Grey level histograms at the surface 7B for the several samples.

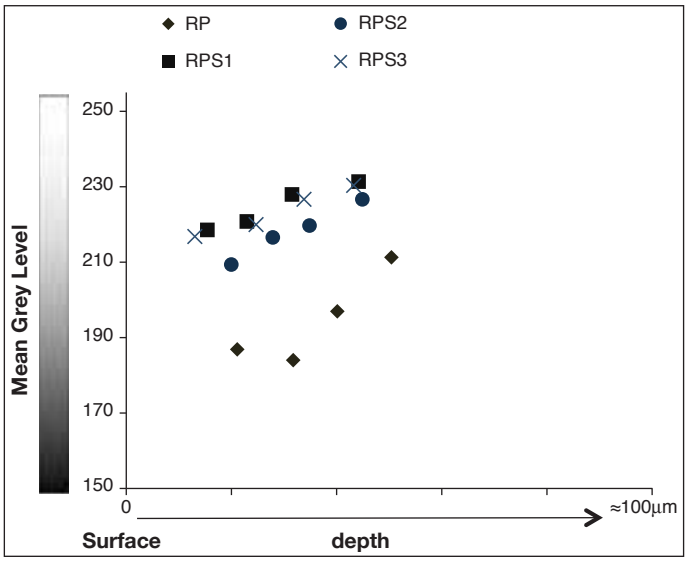

Fig. 11 Graphical representation of the mean grey level values along the z direction of the paper sheets (values obtained at the top surface layer were excluded for better visualization of the differences among the inner layers).

same trend to those of the surface 7B along the several paper samples.

For all the layers (excluding the top surface layer) the skewness value is negative, confirming that the probability curve is skewed to lower grey levels (black regions).

2. Relation between ink pigment penetration and surface treatment

In order to compare the ink pigment penetration for the distinct samples, a plot of the mean grey level values as a function of depth is presented in Figure 11. From this plot it can be concluded that the degree of ink penetration is as follows: RPS1 ≤ RPS3 < RPS2 << RP.

As mentioned in the experimental section, for each surface sized paper sample two additional black printed areas were analysed and the results of the replicates, presented in appendix (Fig. S1) are not markedly different to the initial results.

For a better understanding of the differences in the ink pigment penetration among the several paper samples studied, some surface parameters of the paper sheets were additionally determined, as detailed in Table 3.

The RP sample has the highest water contact angle since no surface treatment was used to increase the hydrophilic character of the surface. When comparing the surface sized samples, water contact angles are much higher for samples RPS2 and RPS3 than for sample RPS1 (Table 3), with the highest value being obtained for sample RPS2. On the other hand, the trend of the polar component of the surface energy is in line with the values from the water contact angles measurements (RPS2< RPS3< RPS1). These results are certainly related to the presence of the copolymers and cationic starch at the sheet surface. It should be kept in mind that the surface sizing agents are located mostly at the top surface, as previously confirmed by FT-IR (*20*). Polymers containing high amount of OH groups, such as cationic starch, or the copolymer poly(styrene-co-acrylate), when located at the sheet surface, may provide hydrogen bonding with water molecules, thus reducing the corresponding contact angle. This is more pronounced for the paper surface sized only with cationic starch (RPS1) than for that surface sized with a mixture of cationic starch/poly(styrene-co-acrylate) (RPS3). For the paper sample RPS2, the presence of the even less polar copolymer, poly(styrene-co-maleic anhydride), renders the surface more hydrophobic than those of RPS1 or RPS3. Similar structural effects are responsible for the increase of the polar component of the surface energy after the surface sizing.

From the ink pigment penetration studies, RPS1 and RPS3 are those samples in which the ink penetrates less in the z direction of the sheet, with sample RP showing the most. Thus, the increase in the ink penetration degree follows the order of decreasing surface polarity. This trend is presumably due to the presence of oxygen-containing groups at the surface of the carbon black particles present in the black ink formulation. These polar groups when interacting with the polar cationic starch or poly(styrene-co-acrylate) macromolecules should be responsible for the high retention of ink pigments at the paper surface and, thus, to the lower ink penetration observed for paper samples RPS1 and RPS3. As for sample RPS2, the surface energy polar component is lower than those of RPS1 and RPS3 and so the ink pigment is less retained at the surface, as confirmed by the grey level histograms. The reference paper is the one in which ink pigment penetrates deeper in the paper structure, as a consequence of hav-

Table 3
Water contact angles, surface energy and porosity for the different paper samples

Sample	Water contact angle, °	Surface Energy Polar Component mN/m	Surface Energy mN/m	Polar/Total Surface Energy	Porosity (%)[a]
RP	101.9 ± 2.2	<0.1	39.5	<0.01	54.1
RPS1	30.3 ± 1.5	75.1	78.1	0.96	56.7
RPS2	68.7 ± 1.6	21.0	34.6	0.61	56.4
RPS3	55.2 ± 0.8	41.1	48.2	0.85	55.1

[a] Obtained by mercury intrusion porosimetry.

ing the less polar surface. It is also possible that the lower surface topographical uniformity predicted for sample RP, in comparison to those of the surface sized samples, may also contribute to the significantly higher ink pigment penetration observed for sample RP. It should be noted that the porosities (measured by mercury intrusion porosimetry) for all paper samples were very similar (between 54-57%, Table 3), and, consequently, this parameter alone, should not influence the different ink penetration results.

CONCLUSION

The ink pigment penetration in different paper samples, containing different surface sizing agents (including the paper sample without surface sizing), was evaluated and compared. From the grey level histograms and the corresponding mean grey level values of the printed samples, it was verified that most of the ink, as expected, was retained at the surface in all cases. Nevertheless, the influence of the surface sizing agents on the ink penetration could be observed. The sample surface sized only with cationic starch (RPS1) was the one in which ink penetrated the least, i.e. was more retained at the surface. This was attributed mainly to the large polar component of the surface energy of the RPS1 sample, making the retention of ink polar groups at the surface higher (thus, lowering the ink penetration degree). The sample without chemical surface sizing (RP) was the one in which ink penetrated the most, showing more ink in the internal layers, located down to about 50 µm (in the z direction) from the printed sheet surface. This behaviour was related mainly to the high RP hydrophobicity. The other samples, RPS2 and RPS3, surface sized with a mixture containing both cationic starch and copolymers had an intermediate behaviour between samples RP and RPS1. Overall, it is believed that chemical and surface energy parameters are decisive, when comparing the effect of the surface sizing on the ink pigment penetration.

Finally, it should be stressed that this work demonstrates that the analysis of the grey level histograms at different depths of printed paper sheets is most helpful to study the influence of the surface sizing treatment on the printing quality.

REFERENCES

(*1*) Hladnik, A., Cernic, M. and Bukosek, V. – Role of paper coating pigments and additives in darkfastness of ink jet prints, *J. Imaging Sci. Techn.* **52**(1):010507-010507-7 (2008).

(*2*) Nilsson, H. and Fogden, A. – Inkjet print quality on model paper coatings, *Appita J.* **61**(2):120-127 (2008).

(*3*) Eriksen, Ø. and Gregersen, Ø.W. – The influence of ink pigment penetration and paper structure on print through, *Nord. Pulp Pap. Res. J.* **20**(2):242-246 (2005).

(*4*) Eriksen, Ø. and Gregersen, Ø. – Ink pigment location measured as the position of clay in yellow coldset ink, *Nord. Pulp Pap. Res. J.* **21**(4):460-465 (2006).

(*5*) Eriksen, Ø. and Gregersen, Ø.W. – The influence of ink oil on print through, *Nord. Pulp Pap. Res. J.* **22**(3):364-370 (2007).

(*6*) Vikman, K. – Fastness properties of ink jet prints on coated papers-part 1: effect of coating polymer system on light fastness. *J. Imaging Sci. Techn.* **47**(1):30-37 (2003).

(*7*) Vikman, K. – Fastness properties of ink jet prints on coated papers-part 2: effect of coating polymer system on water fastness. *J. Imaging Sci. Techn.* **47**(1):38-43 (2003)

(*8*) Vikman, K. and Vuorinen, T. – Light fastness of ink jet prints on modified conventional coatings, *Nord. Pulp Pap. Res. J.* **19**(4):481-488 (2004).

(*9*) Vikman, K. and Vuorinen, T. – Water fastness of ink jet prints on modified conventional coatings, *J. Imaging Sci. Techn.* **48**(2):138-147 (2004).

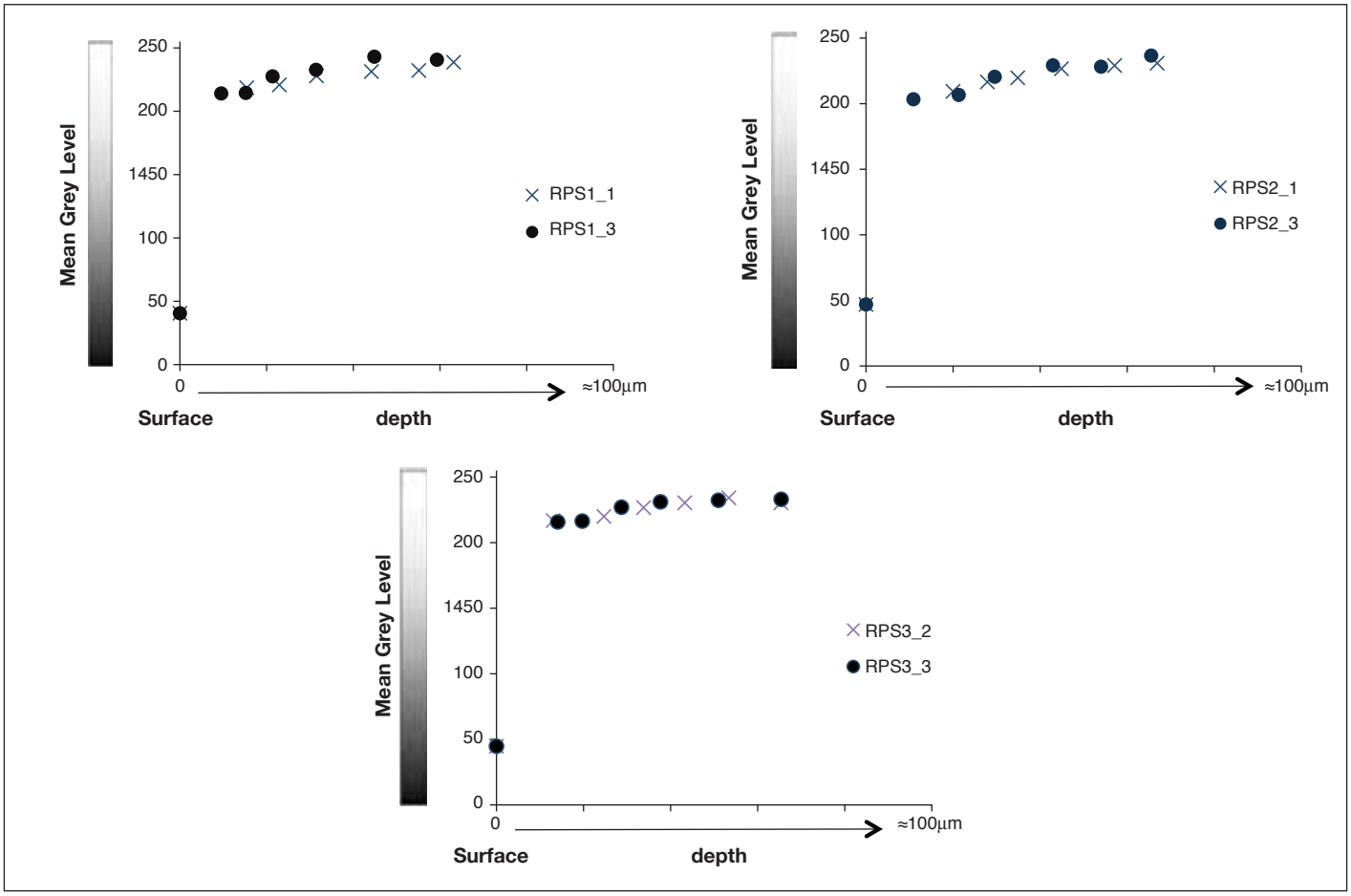

Fig. S1 Graphical representation of the mean grey level values along the z direction of the paper sheets for two replicates of RPS1, RPS2, and RPS3.

(*10*) Xu, R., Fleming III, P.D., Pekarovicova, A. and Bliznyuk, V. – The effect of ink jet paper roughness on print gloss, *J. Imaging Sci. Techn.* **49**(6):660-666 (2005).
(*11*) Lee, H., Joyce, M.K. and Fleming, P.D. – Influence of pigment particle size and pigment ratio on printability of glossy ink jet paper coatings, *J. Imaging Sci. Techn.* **49**(1):54-60 (2005).
(*12*) Lee, H., Joyce, M.K., Fleming, P.D. and Cawthorne, J.E. – Influence of silica and alumina oxide on coating structure and print quality of ink-jet papers. *Tappi J.* **4**(2):11-16 (2005).
(*13*) Sreekumar, J., Sain, M., Farnood, R. and Dougherty, W. – Influence of styrene maleic anhydride imide on inkjet print quality and coating structure, *Nord. Pulp Pap. Res. J.* **22**(3):307-313 (2007).
(*14*) Gregersen, Ø. W, Johnsen, P.O. and Helle, T.J. – Small scale topographical variations of newsprint surfaces and their effects on printing ink transfer distribution, *J. Pulp Pap. Sci.* **21**(10):331-336 (1995).
(*15*) Sequera, J. – Encolado superficial para hacer papeles más competitivos, *El Papel* 50-52 (1999).
(*16*) Pruszynski, P. – Recent developments in papermaking chemicals, Keynote lectures, *Wood Pulp and Paper Conference*, Bratislava, Slovack Republic, p. 82-90 (2003).
(*17*) Shirazi, M., Esmail, N., Garnier, G. and van de Ven, T.G.M. – Starch penetration into paper in a size press, *Proc. 5th International Paper and Coating Symposium*, Montreal, Canada, p. 63-71 (2003).
(*18*) Prinz, M. and Schultz, W.-S. – Sizing agents for surface and wet end application, *Prof. Papermaking* 1, 44-49 (2007).
(*19*) Moutinho, I.M.T., Ferreira, P.J.T. and Figueiredo, M.L. – Impact of surface sizing on inkjet printing quality, *Ind. Eng. Chem. Res.* **46**(19):6183-6188 (2007).
(*20*) Ferreira, P.J., Gamelas, J.A., Moutinho, I.M., Ferreira, A.G., Gómez, N., Molleda, C. and Figueiredo, M.M. – Application of FT-IR-ATR spectroscopy to evaluate the penetration of surface sizing agents into the paper structure, *Ind. Eng. Chem. Res.* **48**(8):3867-3872 (2009).
(*21*) Chinga, G., Eriksen, Ø. and Eilertsen, M. – On the suitability of desktop scanners for assessing print-through, *J. Pulp Pap. Sci.* **33**(3):1-8 (2007).
(*22*) Moutinho I., Figueiredo, M. and Ferreira, P. – Evaluating the surface energy of laboratory-made paper sheets by contact angle measurements, *Tappi J.* **6**(6):26-32 (2007).
(*23*) Owens, D.K. and Wendt, R.C. *J. Appl. Polym. Sci.* **13**(8):1741 (1969).
(*24*) Moura, M.J., Ferreira, P.J. and Figueiredo, M.M. – Mercury intrusion porosimetry in pulp and paper technology, *Powder Technol.*, **160**(2):61-66 (2005).

Original manuscript received 11 September 2009, revision accepted 5 March 2010

Continued from page 363

(*2*) Uimonen, J. and Hättich, T. – Chemical treatment to extend machine clothing and improve water removal – Part I and II, *Proc. of PITA Water removal conference*, York, England, p.57 (1999)
(*3*) Hubbe, M.A., Rojas, O.J. and Venditti, R.A. – Control of tacky deposits on paper machines - A review, *Nord. Pulp Pap. Res. J.* **21**(2):154 (2006)
(*4*) Sihvonen, A-L., Sundberg, K., Sundberg, A. and Holmbom, B. – Stability and deposition tendency of colloidal wood resin, *Nord. Pulp Pap. Res. J.* **13**(1):64 (1998)
(*5*) Welkener, U., Hassler, T. and McDermott, M. – Effect of furnish components on depositability of pitch and stickies, *Nord. Pulp Pap. Res. J.* **8**(1):223 (1993)
(*6*) Guéra, N., Schoelkopf, J. and Gane, P.A.C. – Comparing colloidal pitch adsorption on different talcs, *Nord. Pulp Pap. Res. J.* **2**(20):156 (2005)
(*7*) Mosbye, J., Richardson, D. and Parsons, T. – Solving pitch deposit problems on paper machines using mechanical pulp, *Proc. of 62nd Appita Ann. Conf.* p.185 (2008)
(*8*) Hättich, T., Angle, C.D. and Knight, P. – A novel and effective method to manage contaminants in packaging papermaking, *Paper & Timber* **84**(7):458 (2002)
(*9*) Dechandt, A., Watkins, T., and Pruszynski, P. – Total approach to deposit control on newsprint machine using TMP and DIP pulp mix – from specialized fixation of individual pulps to retention, *Proc. of 57th Appita Ann. Conf.* p.211 (2003)
(*10*) Sawamura, T. – Improving newsprint machine runnability at Iwanuma mill, Japan, *Pap. Tech.* **44**(2):29 (2003)
(*11*) Simons, B., Santos, C. and Meier, M. – Improving productivity through microbial deposit control management, *Pap. Puu* **86**(5):349 (2004)
(*12*) Ekman, J., Kosonen, M., Jokela, S., Kolari, M., Korhonen, P. and Salkinoja-Salonen, M. – Detection and quantitation of colored deposit-forming Meiothermus spp. in paper industry processes and end products, *J. Ind. Microbiol. Biotechnol.* **34**(3):203 (2007)
(*13*) Lahtinen, T., Kosonen, M., Tiirola, M., Vuento, M. and Oker-Blom, C. – Diversity of bacteria contaminating paper machines, *J. Ind. Microbiol. Biotechnol.* **33**(9):734 (2006)
(*14*) Kolari, M. – Attachment mechanisms and properties of bacterial biofilms on non-living surfaces, dissertation, University of Helsinki, Finland (2003)
(*15*) Kanto-Öqvist, C. – Microbial Life and Deposits in Paper Machine Circuits, dissertation, University of Helsinki, Finland (2008)
(*16*) Helle, T. – Characterisation and removal of gas in papermaking, dissertation, Helsinki University of Technology, Finland (2008)
(*17*) Wathén, R. – Requirements for improved runnability at papermachines and in printing, *ipw* (5):58 (2007)
(*18*) Roisum, D.R. – Runnability of paper. Part 1: predicting runnability, *Tappi J.* **73**(1):97 (1990)
(*19*) Roisum, D.R. – Runnability of paper. Part 2: troubleshooting web breaks, *Tappi J.* **2**(73):101 (1990)
(*20*) Malcolm, T. – Proactive break prevention on PM14 at Aylesford Newsprint, *Pap. Tech.* **46**(9):38 (2005)
(*21*) Smith, R.D. (ed.) – **Roll and Web Defect Terminology**, 2nd edition : TAPPI Press (2007)
(*22*) Koskinen, T., Kosonen, M. and Ebeling, K. – The impact of paper defects on paper strength requirements, *Proc. of 12th Fundamental Res. Symp.*, Oxford, UK, p.1441 (2001)
(*23*) Kallio, T. and Kekkonen, J. – Fouling in the paper machine wet end, *Tappi J.* **4**(10):20 (2005)
(*24*) Landry, H.J. – Identification of sheet hole and defects in newsprint mills, *Proc. of TAPPI Newsprint Forum*, Birmingham, Alabama. (1997)
(*25*) Uesaka, T., Ferahi, M., Hristopulos, D., Deng, N. and Moss, C. – Factors controlling press-room runnability of paper, *Proc. of 12th Fundamental Res. Symp.*, Oxford, UK, p.1423 (2001)
(*26*) Väisänen, O.M., Nurmiaho-Lassila, E.L., Marmo, S.A. and Salkinoja-Salonen, M.S. – Structure and Composition of Biological Slimes on Paper and Board Machines, *Appl. Environ. Microbiol.* **60**(2):641 (1994)
(*27*) Peltola, M., Kanto-Öqvist, C., Ekman, J., Kosonen, M., Jokela, S., Kolari, M., Korhonen, P. and Salkinoja-Salonen, M.S. – Quantitative contributions of bacteria and of Deinococcus geothermalis to deposits and slimes in paper industry, *J. Ind. Microbiol. Biotechnol.* **35**(12):1651 (2008)
(*28*) Peltola, M., Neu, T.R., Raulio, M., Kolari, M. and Salkinoja-Salonen, M.S. – Architecture of Deinococcus geothermalis biofilms on glass and steel: a lectin study, *Environ Microbiol.* **10**(7):1752 (2008)

Original manuscript received 23 March 2010, revision accepted 10 June 2010